Effects of Oxidation State, Solvent Acidity and Thiophenol on the Electrochemical Properties of Iron–Molybdenum Cofactor from Nitrogenase

FRANKLIN A. SCHULTZ*[a], BENJAMIN J. FELDMAN[b], STEPHEN F. GHELLER[c] and WILLIAM E. NEWTON*[b,c]

[a]*Department of Chemistry, Purdue University School of Science, Indiana University–Purdue University at Indianapolis, Indianapolis, IN 46205 (U.S.A.)*
[b]*USDA/ARS Western Regional Research Center, Albany, CA 94710 (U.S.A.)*
[c]*Department of Agronomy and Range Science, University of California, Davis, CA 95616 (U.S.A.)*

(Received September 12, 1989)

Abstract

Electrochemical examination of the iron–molybdenum cofactor (FeMoco) extracted from the MoFe protein of *Azotobacter vinelandii* nitrogenase reveals that this important biological cluster exists in a variety of chemical forms whose numbers, proportions and properties depend on oxidation state, *N*-methylformamide solvent acidity and presence of thiophenolate ion. The distribution of oxidized (ox) species, determined from voltammetric responses, and of semi-reduced (s-r) species, determined from EPR spectra, show that FeMoco exists as a 2:1 proportion of populations in its ox state in alkaline NMF and in its ox and s-r states in acidic NMF. A single form of FeMoco(s-r) is found in alkaline NMF. Addition of thiophenol converts all populations of FeMoco into single PhS^--coordinated ox and s-r species under all conditions; these forms exhibit quasi-reversible [FeMoco(ox)-SPh] + e^- $\rightleftharpoons$ [FeMoco(s-r)-SPh] electrochemistry. The variety of cofactor species observed is attributed to various states of ligation, protonation or structural arrangement of the metal cluster. The greater distribution of forms observed in the absence versus presence of thiophenol, in acidic versus alkaline solvent and in the oxidized versus semi-reduced oxidation state suggests that FeMoco exhibits greater structural or compositional heterogeneity under the former of each of these conditions.

Introduction

Iron–molybdenum cofactor (FeMoco) is the Fe, Mo and S-containing cluster that can be extruded from the MoFe protein of nitrogenase and which is now recognized as the site at which dinitrogen is reduced to ammonia by biological systems [1, 2]. An important function of FeMoco is to transfer electrons to the substrate. Thus, to complement ongoing investigations [3–13] of the cofactor's structural, spectroscopic and reactivity properties following extrusion from its protein matrix, we have initiated [13–16] electrochemical studies of isolated FeMoco to provide a better understanding of its role in the mechanism of nitrogen fixation.

The basic aspects of FeMoco electrochemistry in *N*-methylformamide (NMF) are summarized in eqns. (1) and (2). Our previous investigations established this sequence of electron transfer behavior and provided the following additional information regarding the oxidized (ox), semi-reduced (s-r) and fully reduced (red) states of cofactor. (i) Although stored in the presence of excess sodium dithionite to stabilize the semi-reduced oxidation state, and prevent attack by extraneous O_2, FeMoco(s-r) undergoes 'spontaneous oxidation' with time to its oxidized level [15]. (ii) From this state FeMoco is reduced by two sequential electron transfers at −0.3 and −1.0 V versus NHE. The first reduction (eqn. (1)) converts EPR-silent FeMoco(ox) to FeMoco(s-r), which is the state responsible for the biologically unique $S = 3/2$ EPR signal of nitrogenase. Equation (2) produces the fully reduced form of cofactor, which may correspond to the substrate-reducing level of the enzyme [14, 15]. (iii) FeMoco exists in multiple forms in both its (ox) and (s-r) oxidation states. The number and kind of these forms are functions of the acid content of the solvent (NMF) [13, 14]. (iv) Controlled potential coulometry and chemical redox titrations verify that the electron stoichiometry of eqn. (1) is one, even when multiple forms of FeMoco(ox) and FeMoco(s-r) are present [16].

$$\underset{(S=0)}{\text{FeMoco(ox)}} + e^- \rightleftharpoons \underset{(S=3/2)}{\text{FeMoco(s-r)}} \qquad (1)$$

$$\underset{(S=3/2)}{\text{FeMoco(s-r)}} + ne^- \rightleftharpoons \text{FeMoco(red)} \qquad (2)$$

*Authors to whom correspondence should be addressed.

0020-1693/90/$3.50

This manuscript presents the results of a detailed electrochemical characterization of the (ox)/(s-r) couple of FeMoco obtained from *Azotobacter vinelandii* nitrogenase. More extensive examination of this redox system was prompted by two considerations. First, we are planning to carry out X-ray absorption spectroscopic experiments under electrochemically controlled conditions to determine if changes in structure accompany reduction/oxidation of FeMoco. Accurate and complete electrochemical information is needed to conduct these experiments successfully, particularly in the presence of multiple forms. Second, our initial investigations revealed anomalous behavior (small peak current magnitudes and non-diffusional wave shapes) associated with electrochemical reduction of FeMoco(ox). We wished to learn if these observations could be modeled by the presence of multiple forms of cofactor using standard electrochemical theory. The ability to do so would verify that electrochemistry provides valid information on cofactor properties and can be used with confidence in further investigations of this material.

Experimental

Materials and Methods

MoFe protein of *A. vinelandii* nitrogenase was isolated and purified and FeMoco released into NMF by previously published methods [11b, 17]. All FeMoco samples were concentrated by vacuum evaporation and stored anaerobically at −80 ℃ until used [15]. Mo and Fe contents were determined spectrophotometrically using toluene-3,4-dithiol and *o*-phenanthroline, respectively; samples had an average of 6.15 ± 0.11 Fe atoms per Mo [11b, 18]. The activity of FeMoco solutions was assayed by reconstituting the acetylene-reducing ability of FeMoco-deficient protein in crude extracts of the DJ35 mutant of *A. vinelandii* [19]. Assays conducted before and after manipulations of FeMoco showed no loss of activity and were within the range of 192 ± 64 nmol acetylene reduced $(\text{min})^{-1}$ (ng atom Mo)$^{-1}$. *N*-Methylformamide (Aldrich) was vacuum distilled immediately prior to use in electrochemical experiments. Solvent that was pretreated by stirring over barium oxide for 18 h before distillation is referred to as 'alkaline'; solvent distilled without such pretreatment is 'acidic'. Acidic solvent was also produced by adding *p*-toluenesulfonic acid (HPTS) to BaO-distilled NMF. 'Alkaline' and 'acidic' NMF gave pH readings of 10–11 and 6–8, respectively, after dilution into 9 parts of water. *p*-Toluenesulfonic acid (Eastman Kodak), thiophenol (Aldrich) and tetra-n-butylammonium hexafluorophosphate ($TBAPF_6$; Southwestern Analytical Chemicals) were used as received. Ferrocene (Aldrich) was sublimed. $[Bu_4N]_3$-$[Mo(S_2C_2(CN)_2)_4]$ was prepared by the literature method [20]. NaSPh was prepared by neutralization of thiophenol with sodium metal.

Electrochemistry

Electrochemical experiments were conducted under an argon or helium atmosphere in a Vacuum Atmospheres glove box. Construction of the electrochemical cells used in these experiments is described elsewhere [15, 16, 21]. A microcell containing a 0.071 cm^2 glassy carbon (GC) working electrode was used to examine small volumes (40–70 μl) of undiluted FeMoco solutions. A larger cell of *c.* 2 ml capacity containing a large surface area reticulated vitreous carbon (RVC) working electrode was used to examine diluted solutions of FeMoco and to carry out bulk electrolysis experiments. In the RVC cell, experiments were conducted by adding aliquots of FeMoco to 1 ml of NMF containing 0.1 M $TBAPF_6$ sufficient to give final Mo concentrations of 0.05 to 0.5 mM. Potentials were measured against an aqueous Ag/AgCl (3 M NaCl) reference electrode and converted to the normal hydrogen electrode (NHE) scale using either the ferrocene/ferricenium or $[Mo(S_2C_2(CN)_2)_4]^{3-/4-}$ redox couples as described previously [15, 16]. Electrochemical experiments were conducted with a CV-27 potentiostat (Bioanalytical Systems) which was connected to the cells by shielded cable passed through an air-tight seal in the glove box.

Digital simulations were carried out with programs based on those described by Feldberg [22]. The programs were executed on an Everex 1800 microcomputer using Microsoft Fortran 4.1. We thank Professor W. E. Geiger for copies of these programs.

Results

Results in Alkaline NMF

The open circles in Fig. 1(a) describe a background-corrected cyclic voltammogram recorded at a sweep rate of 40 mV s^{-1} for reduction of FeMoco(ox) (0.138 mM in Mo) at an RVC electrode in BaO-distilled ('alkaline') NMF containing 0.1 M $TBAPF_6$. Under these conditions, FeMoco(ox) reduction exhibits a formal potential of $E^{\circ\prime} = -0.36$ V versus NHE and has many characteristics of a diffusion-controlled electrode reaction. The cathodic peak current is proportional to the square root of sweep rate (for $\nu = 10$ to 100 mV s^{-1}) and to FeMoco concentration (for $C = 0.1$ to 0.5 mM). The separation between cathodic and anodic peak potentials is 145 mV. This relatively large value results in part from the uncompensated *iR* drop incurred by use of a large surface area working electrode, but because the magnitude of ΔE_p is significantly greater than the value exhibited by a kinetically facile one-electron

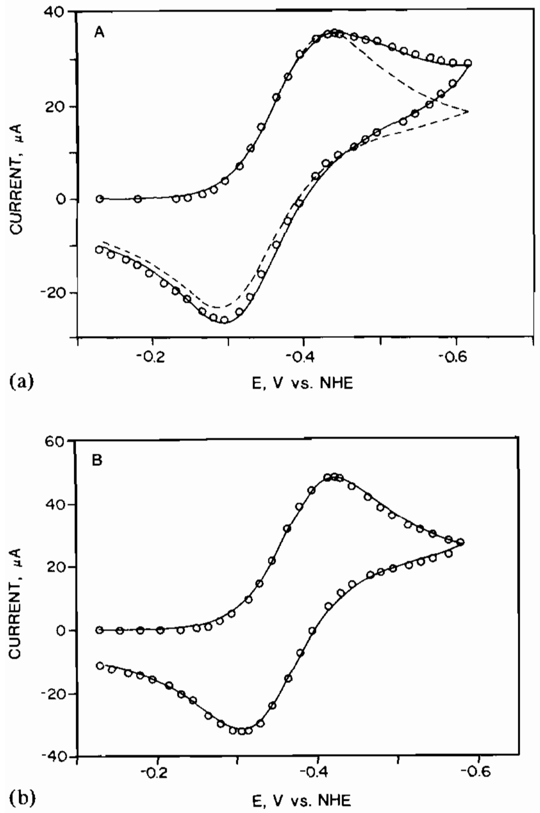

Fig. 1. Comparison of experimental and digitally simulated cyclic voltammograms for reduction of FeMoco(ox) in alkaline NMF containing 0.1 M $TBAPF_6$ at RVC electrode. (a) Experimental points for reduction of 0.138 mM FeMoco(ox) at $\nu = 40$ mV s^{-1} (open circles); digitally simulated reduction of a single component with $E^{\circ\prime} = -0.355$ V, $k_{s,h}/D^{1/2} = 0.533$ $s^{-1/2}$, $\alpha = 0.50$ (broken line); digitally simulated reduction of a three-component mixture consisting of a 60:20:20 distribution of species with the following characteristics: 60%, $E^{\circ\prime} = -0.355$ V, $k_{s,h}/D^{1/2} = 0.667$ $s^{-1/2}$, $\alpha = 0.50$; 20%, $E^{\circ\prime} = -0.400$ V, $k_{s,h}/D^{1/2} = 0.200$ $s^{-1/2}$, $\alpha = 0.50$; 20%, $E^{\circ\prime} = -0.480$ V, $k_{s,h}/D^{1/2} = 0.0367$ $s^{-1/2}$, $\alpha = 0.50$ (solid line). (b) Experimental points for reduction of 0.132 mM FeMoco(ox) plus 1.19 mM thiophenolate ion at $\nu = 40$ mV s^{-1} (open circles); digitally simulated reduction of a single component with $E^{\circ\prime} = -0.362$ V, $k_{s,h}/D^{1/2} = 0.827$ $s^{-1/2}$, $\alpha = 0.50$ (solid line). Heights of digitally simulated curves are normalized to experimental peak currents in all cases.

transfer under the same experimental conditions (e.g. $\Delta E_p = 80$ mV for $Mo[S_2C_2(CN)_2]_4^{3-}$ reduction at $\nu = 40$ mV s^{-1}), we conclude that a degree of charge transfer irreversibility is associated with FeMoco(ox) reduction at the RVC electrode.

Close inspection of the experimental trace in Fig. 1(a) reveals several abnormalities associated with the voltammetric reduction of FeMoco(ox). (i) The cathodic peak current of 35 μA is significantly smaller than the value expected for a one-electron transfer under these experimental conditions. (ii) The anodic-to-cathodic peak current ratio (evaluated by use of the semi-empirical formula of Nicholson [23]) is greater than unity ($i_{pa}/i_{pc} = 1.23$). (iii) Current at potentials more negative than the cathodic peak does not decrease as rapidly as expected for a diffusion-controlled electrode reaction. Points (ii) and (iii) are illustrated by comparison of the experimental curve with a digitally simulated cyclic voltammogram of a single component (broken line) whose electrochemical parameters ($E^{\circ\prime} = -0.355$ V, $k_{s,h}/D^{1/2} = 0.533$ $s^{-1/2}$, $\alpha = 0.50$) have been adjusted to give the same peak potentials as the experimental trace.

The realization (*vide infra* and refs. 13 and 14) that FeMoco(ox) samples in 'acidic' NMF exhibit, at more negative potentials, additional voltammetric reduction peaks, which correspond to approximately one-third the FeMoco content of the solution, suggests that a similar distribution might exist in the 'alkaline' solvent also. If the species responsible for these peaks were to undergo electrochemical reduction more sluggishly under alkaline conditions, they could contribute to the diminished cathodic peak current and flattened wave shape without appearing as distinct maxima. To model this behavior, we carried out digital simulation of a mixture of three forms of FeMoco(ox) consisting of 60% material having the same electrochemical parameters that defined the broken line in Fig. 1(a) and 20% each of two additional forms having standard electrode potentials of -0.400 and -0.480 V and electrochemical rate parameters of $k_{s,h}/D^{1/2} = 0.200$ and 0.0367 $s^{-1/2}$, respectively. The solid line in Fig. 1(a) shows the agreement between this simulation and the experimental trace. The additional species adequately account for the slow decrease in current following the cathodic peak and the additional anodic current on the positive sweep of the cyclic voltammogram. While we do not place great reliance on the quantitative nature of the parameters obtained from this fit, the simulation shows that the anomalous characteristics of FeMoco(ox) reduction in alkaline NMF can be accounted for by a fraction of material that is sluggishly reduced at more negative potentials.

Figure 1(b) illustrates the cyclic voltammetric behavior of the solution in Fig. 1(a) after addition of 1.19 mmol per liter of NaSPh. Addition of excess thiophenolate ion has three effects on the experimental response (open circles). (i) The peak current of the principal FeMoco(ox) reduction wave increases from 35 to 48 μA. (ii) The current following the cathodic peak decreases more rapidly with increasing negative potential. (iii) The anodic-to-cathodic peak current ratio becomes unity ($i_{pa}/i_{pc} = 1.02$). The solid line in Fig. 1(b) demonstrates that the experimental trace can now be simulated by diffusion controlled reduction of a single species with electrochemical parameters of $E^{\circ\prime} = -0.362$ V, $k_{s,h}/D^{1/2} = 0.827$ $s^{-1/2}$ and $\alpha = 0.50$.

In previous work [11a], we determined from the narrowing of the $S = 3/2$ EPR signal of semi-reduced cofactor during titration with thiophenol, that this reagent (when added either as PhSH or PhS^-) forms a 1:1 complex with FeMoco(s-r). Figure 1(b) is evidence that thiophenolate ion binds to the oxidized form of cofactor also and, in so doing, converts the mixture of species present into a single form. The FeMoco(ox) reduction potential remains independent of PhS^- concentration when thiophenolate ion is in excess of FeMoco and its concentration is varied. Therefore, we conclude that, in both oxidation states, cofactor is bound to a single PhS^- ligand and that its ox to s-r reduction under these conditions can be assigned to electrode reaction (3).

$$\text{FeMoco(ox)-SPh} + e^- \rightleftharpoons \text{FeMoco(s-r)-SPh} \qquad (3)$$

Binding of thiophenol to ox and s-r cofactor has also been demonstrated by ^{19}F NMR of p-$CF_3C_6H_4S^-$ treated FeMoco [24].

Results in Acidic NMF

Figure 2(a) illustrates the cyclic voltammetric response of an oxidized cofactor sample that has not been diluted into NMF following isolation. We find that the acidity of the solvent in these undiluted samples is always higher than that of NMF that has been freshly distilled from barium oxide*. Figure 2a shows that two distinct cathodic peaks (C′ and C″) are observed at potentials *c.* 150 and 300 mV more negative than the principal FeMoco(ox) reduction wave (A). Peaks C′ and C″ appear to correspond to the minor components of oxidized cofactor solution (Fig. 1(a)) whose reduction becomes more evident in acidic solvent. In addition, the $E^{\circ\prime}$ of the principal FeMoco(ox) reduction wave is shifted to −0.31 V by the change to acid conditions. Similar results are obtained if FeMoco(ox) is diluted into undistilled NMF (which we find to be acidic) or into BaO-distilled NMF subsequently made acidic by addition of HPTS. Figure 2(b) illustrates the result of the latter experiment in which case only a single additional reduction peak is observed at more negative potentials.

Figure 2(c) shows the result of adding a seven-fold molar excess of PhSH to FeMoco(ox) in acidic NMF. This addition results in disappearance of the additional waves at more negative potentials and an increase in current of the principal reduction wave from 5.0 to 8.9 μA. The formal reduction potential

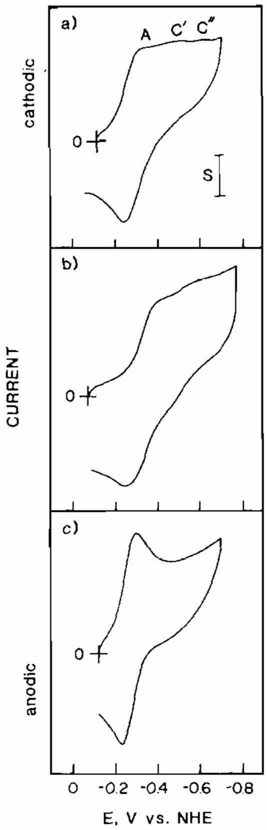

Fig. 2. (a) Cyclic voltammetric reduction of 2.84 mM FeMoco(ox) in undiluted, acidic NMF at GC electrode, $\nu = 40$ mV s^{-1}. Peaks A, C′ and C″ correspond to similarly labelled plots of peak potential vs. sweep rate in Fig. 4. $S = 2$ μA. (b) Cyclic voltammetric reduction of 0.142 mM FeMoco(ox) in 0.1 M $TBAPF_6$/NMF at an RVC electrode after addition of 0.99 mmol l^{-1} of HPTS. $\nu = 40$ mV s^{-1}, $S = 5$ μA. (c) Cyclic voltammetric reduction of sample in Fig. 2a after addition of 21 mmol l^{-1} of PhSH. $\nu = 40$ mV s^{-1}, $S = 2$ μA.

(−0.36 V) is the same as that observed in alkaline NMF and is independent of excess thiophenol concentration. Thus, addition of excess PhSH to FeMoco(ox) in acid NMF appears to generate the same FeMoco(ox)-SPh species that is formed in alkaline NMF and whose electrochemical reduction is described by eqn. (3).

Figure 3 contains plots of peak current versus the square root of sweep rate for the first reduction wave of an undiluted 2.84 mM FeMoco(ox) sample alone and after addition of a seven-fold molar excess of PhSH. Both plots display the expected linear response of peak current upon $\nu^{1/2}$ although the plot for FeMoco(ox) reduction in the absence of PhSH exhibits a negative deviation above 0.1 V s^{-1}. The slopes in the absence and presence of thiophenol are 26 and 44 μA $s^{1/2}$ $V^{-1/2}$, respectively. The ratio between these slopes (0.6) is approximately the same as the ratio between peak currents (0.7) for reduction

*The reason for the difference in acidity has not been established. Impurities introduced by various steps in the FeMoco isolation procedure or chemical reactions during its storage could account for the acidic character of undiluted samples. BaO-catalyzed decomposition of solvent could account for the basic character of NMF distilled from this reagent.

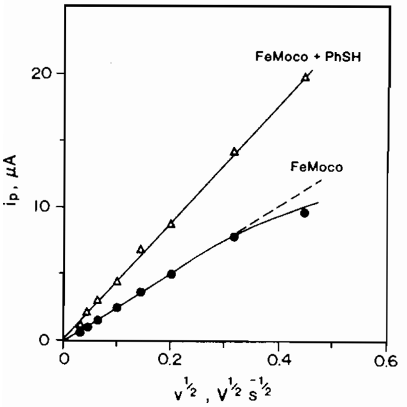

Fig. 3. Plots of peak current vs. square root of sweep rate for reduction of 2.84 mM FeMoco(ox) in undiluted acidic NMF at GC electrode; alone (●) and in the presence (△) of 0.021 M PhSH. Currents in the presence of PhSH are corrected for dilution.

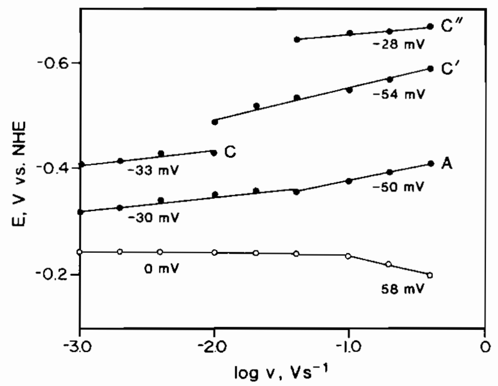

Fig. 4. Plots of cathodic (●) and anodic (○) peak potentials as a function of sweep rate from cyclic voltammetry of FeMoco(ox) in undiluted, acidic NMF. Letters refer to the major (A) and minor (C, C′, C″) forms of FeMoco(ox) in acid NMF. Numbers are the slope of $\Delta Ep/\Delta \log \nu$ in mV for the corresponding linear segment.

of an alkaline FeMoco(ox) sample in the absence and presence of PhS^- (Fig. 1). Assuming that thiophenol converts all forms of FeMoco(ox) into a single electrochemically active FeMoco(ox)-SPh species under both conditions, this result indicates that the fraction of material associated with the principal FeMoco(ox) reduction wave is *c.* 2/3 in both acid and alkaline NMF. The remaining one-third of FeMoco(ox) appears to be accounted for by one or more species that undergo reduction sluggishly at potentials slightly more negative than the principal reduction wave. These species cannot be in rapid equilibrium with the major fraction of FeMoco(ox), because as illustrated by the behavior in acidic NMF, diffusion-limited i_p versus $\nu^{1/2}$ response for the first reduction wave is maintained down to a sweep rate of 0.001 V s^{-1} (Fig. 3).

Plots of peak potential versus sweep rate in Fig. 4 further illustrate the distribution of subspecies within the minor fraction of FeMoco(ox) in acidic NMF. Plot A represents the peak potential for reduction of the single major form that is observed at all sweep rates. Plots C′ and C″ represent peak potentials for the reduction of two minor forms of FeMoco(ox) in acidic NMF that were identified in Fig. 2(a). The peaks for these processes vanish at sweep rates below 0.01 V s^{-1} and are replaced by a single peak (C) at slightly more positive potentials. The E_p versus log ν response of this species does not coincide with that of C′, C″ or A. Thus, we conclude that the minor fraction of acidic FeMoco(ox) consists of at least three identifiable subspecies (C, C′ and C″) two of which (C′ and C″) condense into a third form (C) as sweep rate is decreased, and all of which react independently of the single major form (A) at the electrode surface. A similar distribution of subspecies may exist within the minor fraction of FeMoco(ox) in alkaline NMF, but this point is difficult to establish because of its sluggish electrochemical response. However, satisfactory simulation of experimental alkaline voltammograms can be achieved only by including the reduction of at least two minor components at potentials more negative than the principal reduction wave (Fig. 1(b)). These alkaline subspecies are designated D′ and D″ to preserve correspondence with the subspecies C′ and C″ in acidic NMF. Electrochemical response in alkaline NMF is too poorly defined to determine if D′ and D″ coalesce into a separate single form (D) at slow sweep rates.

Formal Potentials and Identification of Species

Table 1 lists the forms of cofactor identified in this work and formal potentials measured for these species under different experimental conditions. The letters A and B represent the major oxidized forms of cofactor in acidic and alkaline media, respectively; the letters C and D represent the minor oxidized forms under the same conditions. Distribution of the minor forms into subspecies is indicated by primed or unprimed symbols. In the semi-reduced oxidation state, R, N and W forms of FeMoco have been identified by EPR spectroscopy [13]. Relationships between these forms and the various forms of oxidized FeMoco also are included in the Table.

Discussion

Evidence for discrete acidity-dependent fractions of oxidized cofactor came initially from EPR spectroscopic experiments which revealed differences in $S = 3/2$ signals following reduction to FeMoco(s-r) [13]. Now our electrochemical experiments also indicate that FeMoco(ox) exists in discrete fractions in acid and alkaline media and that these fractions

TABLE 1. Distribution of species and formal electrode potentials for the FeMoco(ox)/FeMoco(s-r) couple under various solution conditions

Conditions	Oxidized cofactor	Semi-reduced cofactor	$E^{\circ\prime}$ [a]
Alkaline NMF [b]	B	R	-0.36 ± 0.02[d]
	D		not observed
	D′		-0.40[e]
	D″		-0.48[e]
+ PhS^-	FeMoco(ox)-SPh	FeMoco(s-r)-SPh	-0.35 ± 0.01[f]
Acidic NMF [c]	A	N	-0.31 ± 0.01[g]
	C	W	-0.34[h]
	C′		-0.39
	C″		-0.44
+ PhSH	FeMoco(ox)-SPh	FeMoco(s-r)-SPh	-0.37 ± 0.01[f]

[a]In V vs. NHE; determined as the average of cathodic and anodic peak potentials from cyclic voltammetric reduction of FeMoco(ox) at 0.04 V s^{-1}. [b]Recorded in 0.1 M $TBAPF_6$/NMF at RVC electrode. [c]Recorded at GC electrode in undiluted NMF. [d]Standard deviation of 28 measurements. [e]From digital simulation in Fig. 1. [f]Average deviation of 2 measurements. [g]Standard deviation of 10 measurements. [h]Recorded at 0.004 V s^{-1}.

have different compositions and/or properties. Evidence for differences in compositions or properties consists of the shift in formal potential of the major reduction wave (A and B) upon solvent acidification and changes in reduction potential and apparent heterogeneous electron transfer rates for the minor oxidized forms (C and D). Interestingly, the factors responsible for generating the different $S = 3/2$ signals of FeMoco(s-r) are not reflected in the electrochemistry of this material. Only a single anodic peak at -0.24 V versus NHE is observed for FeMoco(s-r) oxidation in both alkaline and acidic NMF*. Thus, we find no electrochemical evidence for differentiation of the R, N and W forms of semi-reduced cofactor, although these species exhibit distinct $S = 3/2$ EPR signals.

Scheme 1 summarizes relationships between the oxidized and semi-reduced forms of FeMoco and the manner in which we believe conversions among these species are accomplished by changes in redox state, solvent acidity and the presence of thiophenol or thiophenolate ion. Electrochemical evidence indicates that the B:D and A:C populations of oxidized cofactor exist in approximate 2:1 proportion in alkaline and acidic media, respectively. In acid solution, the A(ox) plus C(ox) population is reduced to corresponding proportions of semi-reduced N(s-r) and W(s-r), whose unique identities and approximate concentrations are established on the basis of their $S = 3/2$ EPR signals [13]. In alkaline solution, the 2:1 distribution of B(ox) plus D(ox) is reduced to a single species, R(s-r), which constitutes the entire population of FeMoco(s-r). Addition of PhSH to acidic NMF or of PhS^- to alkaline NMF consolidates the entire distribution of FeMoco forms present under any set of conditions into single species in both the (ox) and (s-r) oxidation states. These are identified as 1:1 complexes of FeMoco with PhS^- which undergo quasi-reversible one-electron transfer as described by eqn. (3).

*Small secondary peaks, such as that shown at *c.* -0.5 V on the return sweep in Fig. 2(b), are seen in conjunction with FeMoco(s-r) oxidation only when a large molar excess of HPTS is present.

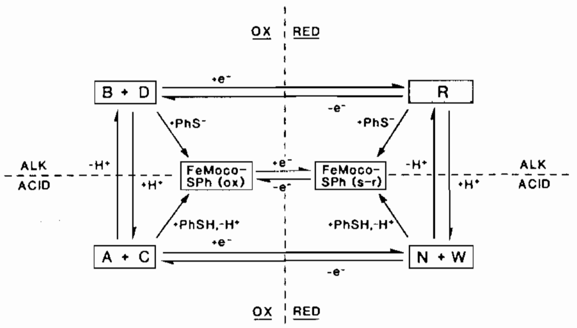

Scheme 1. Oxidized subspecies identified by primed or unprimed symbols are not included; it is assumed that these are reduced as a single population to the corresponding semi-reduced form.

Comments on the Existence of Multiple Forms of FeMoco

While we would like to correlate interconversion of the various forms of FeMoco with events of definite molecular stoichiometry, this is not possible because, despite extensive investigations of the topic the composition and structure of iron–molybdenum cofactor are not completely known. However, electrochemical and EPR spectroscopic results suggest that oxidation state, solvent acidity and the presence of ligating thiophenolate ion guide the distribution of cofactor species.

Detection under all conditions of a single species, which accounts for 100% of the FeMoco content and undergoes quasi-reversible ox to s-r electron transfer, suggests that the thiophenolated form of FeMoco possesses the greatest structural and compositional integrity. Conversely, the greater number of forms observed in the absence versus the presence of thiophenol, in acidic versus alkaline solvent and in the oxidized versus semi-reduced oxidation state indicates that cofactor exhibits greater structural and compositional heterogeneity under the former of each of these conditions. We believe it likely that the various cofactor forms generated by these conditions represent different states of ligation, protonation or structural arrangement of the metal cluster unit. For example, the ability of alkaline versus acidic NMF to extract cofactor from the MoFe protein of *A. vinelandii* nitrogenase has led to the suggestion [11b] that *N*-methylformamidate ion may be a cofactor ligand. The greater number of species observed in acid NMF then would be consistent with the reduced ability of the solvent to function as a ligand under these conditions. Likewise, the ability of thiophenol to consolidate multiple forms of FeMoco into a single species also can be attributed to ligation.

Electrochemical response indicates that structural or compositional differences exist between the ox and s-r states of FeMoco. The strongest evidence of this fact is the smaller number of species observed in the semi-reduced oxidation state. However, the apparent irreversibility of the ox to s-r electrode reaction suggests that changes in structure may accompany this electrochemical process. Figure 4 shows that the peak potentials for FeMoco(ox) reduction shift in the negative direction with increasing sweep rate. This behavior is indicative of either an irreversible charge transfer reaction or a reversible charge transfer followed by an irreversible chemical reaction [25]. Conversely, a single sweep-rate independent peak potential is observed for FeMoco(s-r) oxidation (Fig. 4), which indicates facile electron transfer and minimal structural reorganization in the oxidizing direction. Electrochemical results therefore indicate a much greater structural integrity for FeMoco in its semi-reduced oxidation state.

A final point to consider is the reproducible 2:1 distribution of populations observed for FeMoco(ox) in alkaline and acid NMF and for FeMoco(s-r) in acid NMF. This distribution may reflect particular favored states of structural organization adopted by the Fe–Mo–S cluster upon its release from the protein environment. If such structural or compositional changes (or others induced by changes in acidity or oxidation state) occur upon extraction from the protein, they have only minor effects on the redox and EPR spectroscopic properties of the Fe–Mo–S center and do not diminish the biological activity of cofactor when reconstituted in the protein. However, their influence on the ability of the extracted metal cluster to catalyze substrate reduction reactions has yet to be demonstrated.

Further information on the structure and composition of the various forms of FeMoco will require X-ray absorption and other spectroscopic experiments to be carried out under electrochemical control. Such experiments are underway.

Acknowledgements

The authors gratefully acknowledge support from the National Science Foundation (CHE-87-18013, F.A.S.) and the National Institutes of Health (DK-37255, W.E.N.).

References

1 V. K. Shah and W. J. Brill, *Proc. Natl. Acad. Sci. U.S.A., 74* (1977) 3249.

2 T. R. Hawkes, P. A. McLean and B. E. Smith, *Biochem. J., 217* (1984) 317.

3 B. Hedman, P. Frank, S. F. Gheller, A. L. Roe, W. E. Newton and K. O. Hodgson, *J. Am. Chem. Soc., 110* (1988) 3798.

4 S. D. Conradson, B. K. Burgess, W. E. Newton, L. E. Mortenson and K. O. Hodgson, *J. Am. Chem. Soc., 109* (1987) 7507.

5 S. D. Conradson, B. K. Burgess, W. E. Newton, K. O. Hodgson, J. W. McDonald, J. F. Rubinson, S. F. Gheller, L. E. Mortenson, M. W. W. Adams, P. K. Mascharak, W. A. Armstrong and R. H. Holm, *J. Am. Chem. Soc., 107* (1985) 7935.

6 J. M. Arber, A. C. Flood, C. D. Garner, C. A. Gormal, S. S. Hasnain and B. E. Smith, *Biochem. J., 252* (1988) 421.

7 M. R. Antonio, B.-K. Teo, W. H. Orme-Johnson, M. J. Nelson, S. E. Groh, P. A. Lindahl, S. M. Kauzlarich and B. A. Averill, *J. Am. Chem. Soc., 104* (1982) 4703.

8 H. Thomann, T. V. Morgan, H. Jin, S. J. N. Burgmayer, R. E. Bare and E. I. Stiefel, *J. Am. Chem. Soc., 109* (1987) 7913.

9 D. M. Kurtz, Jr., R. S. McMillan, B. K. Burgess, L. E. Mortenson and R. H. Holm, *Proc. Natl. Acad. Sci. U.S.A., 76* (1979) 4986.

10 J. Rawlings, V. K. Shah, J. R. Chisnell, W. J. Brill, R. Zimmermann, E. Munck and W. H. Orme-Johnson, *J. Biol. Chem., 253* (1978) 1001.

11 (a) B. K. Burgess, E. I. Stiefel and W. E. Newton, *J. Biol. Chem., 255* (1980) 353; (b) S.-S. Yang, W.-H. Pan, D. G. Friesen, B. K. Burgess, J. L. Corbin, E. I. Stiefel and W. E. Newton, *J. Biol. Chem., 257* (1982) 8042.

12 M. A. Walters, S. K. Chapman and W. H. Orme-Johnson, *Polyhedron, 5* (1986) 561.

13 W. E. Newton, S. F. Gheller, B. J. Feldman, W. R. Dunham and F. A. Schultz, *J. Biol. Chem., 264* (1989) 1924.

14 F. A. Schultz, S. F. Gheller, B. J. Feldman and W. E. Newton, in H. Bothe, F. J. deBruijn and W. E. Newton

(eds.), *Nitrogen Fixation: Hundred Years After,* Fischer Verlag, Stuttgart, 1988, pp. 121–126.
15 F. A. Schultz, S. F. Gheller, B. K. Burgess, S. Lough and W. E. Newton, *J. Am. Chem. Soc., 107* (1985) 5364.
16 F. A. Schultz, S. F. Gheller and W. E. Newton, *Biochem. Biophys. Res. Commun., 152* (1988) 629.
17 B. K. Burgess, D. L. Jacobs and E. I. Stiefel, *Biochim. Biophys. Acta, 614* (1980) 196.
18 L. J. Clark and J. H. Axley, *Anal. Chem., 27* (1955) 2000.
19 K. E. Brigle, M. C. Weiss, W. E. Newton and D. R. Dean, *J. Bacteriol., 169* (1987) 1547.
20 D. A. Smith, J. W. McDonald, H. O. Finklea, V. R. Ott and F. A. Schultz, *Inorg. Chem., 21* (1982) 3825.
21 B. J. Feldman, S. F. Gheller, G. F. Bailey, W. E. Newton and F. A. Schultz, *Anal. Biochem.,* (1990), in press.
22 (a) S. W. Feldberg, in A. J. Bard (ed.), *Electroanalytical Chemistry,* Vol. 3, Marcel Dekker, New York, 1969, pp. 199–296; (b) S. W. Feldberg, in J. S. Mattson, H. B. Mark, Jr. and H. C. MacDonald, Jr. (eds.), *Electrochemistry: Calculations, Simulation and Instrumentation,* Vol. 2, Marcel Dekker, New York, 1972, pp. 185–215.
23 R. S. Nicholson, *Anal. Chem., 38* (1966) 1406.
24 S. D. Conradson, B. K. Burgess and R. H. Holm, *J. Biol. Chem., 263* (1988) 13, 743.
25 R. S. Nicholson and I. Shain, *Anal. Chem., 36* (1964) 706.